

Fig. 2. Frequency spectrum of vibrations excited by Gullfoss.

against the base of the fall, details of the transfer of momentum are obscure. It is noteworthy that the slope of the solid line in Fig. 1 is 250 m/sec, about one-fourth the velocity of sound in water, suggesting that the entire water column may be resonating in the quarter wavelength mode. The impedance match at the base of the fall is good whereas that of the top is poor; this would place the node at the brink of the fall.

Water breaks up into discrete turbulent eddies as it falls, with the length of each eddy increasing with distance of fall. Such separation, which would give intermittent impacts and lower frequency with greater height, is clearly evident in most regular waterfalls. A small individual turbulent eddy usually does not maintain its identity the full length of fall. It grows in length and then melds with others to form larger and longer eddies, each of which strikes the base of the fall, producing strong earth motion.

JOHN S. RINEHART

*Environmental Science Services  
Administration, Research Laboratories,  
Boulder, Colorado 80302*

28 February 1969

1514

## Lunar Surface Material: Spacecraft Measurements of Density and Strength

**Abstract.** *The relation of the density of the lunar surface layer to depth is probably best determined from spacecraft measurements of the bearing capacity as a function of depth. A comparison of these values with laboratory measurements of the bearing capacity of low-cohesion particulate materials as a function of the percentage of solid indicates that the bulk density at the lunar surface is about 1.1 grams per cubic centimeter and that it increases nearly linearly to about 1.6 grams per cubic centimeter at a depth of 5 centimeters.*

Despite the successful landing of seven unmanned spacecraft on the moon, controversy continues about the density of lunar surface material. I present here further analysis of the available data.

With the Surveyor 7 soil mechanics surface sampler (1) the density of one surface rock was directly measured as  $2.8 \pm 0.4$  g/cm<sup>3</sup>. From the elemental chemical analyses made on the moon (2), model oxide compositions were derived that correspond to rock densities of 3.2 g/cm<sup>3</sup> in the maria sites of Surveyors 5 and 6, and 3.0 g/cm<sup>3</sup> at the Surveyor 7 site on the rim of Tycho (3). These values, however, pertain to the density of a fragment and of solid rock, rather than to the bulk density of the particulate layer that mantles the lunar surface.

A gamma-scattering densitometer on Luna 13 provided a direct indication of the bulk density. Unfortunately, the curve of density plotted against counting rate was double-valued, and the data fit a bulk density of about 0.8 g/cm<sup>3</sup> or greater than 2.1 g/cm<sup>3</sup> (4, 5). These values pertain to effective depths of 5 to 10 cm (6).

For particulate material of low cohesion, the static bearing capacity is a rather sensitive function of the percentage of solid and hence of the bulk density. Data on the static bearing capacity at various depths in the lunar surface layer are available from determinations of the loads imposed by a number of objects which made imprints on the surface and the corresponding bearing areas. The objects include a small rolling stone near Surveyor 5 (7), the head of the alpha-scattering instrument on Surveyor 7 (8), landing blocks on Surveyors 6 and 7 (8, 9), surface samplers used in bearing tests on Surveyors 3 and 7 (1, 10), a footpad on Surveyor 1 (8, 9), and a boulder that had rolled down the side of the crater Sabine D, as observed from Lunar Orbiter 2 (11). The imprint depth, bearing capacity, and bearing width for each object are shown in

Table 1. The consistency of the Surveyor data is illustrated by a plot of bearing capacity against depth (Fig. 1); the data for width-to-depth ratios of 5 to 10 fall on a straight line through the origin, with a slope of about 1 newton/cm<sup>2</sup>. Data for width-to-depth ratios of 0.8 to 1 fall at slightly lower bearing capacities, as would be expected from ordinary soil mechanics relations. The value for the Lunar Orbiter boulder indicates some decrease in the slope of the curve of bearing capacity versus depth at greater depths, as would be expected.

Laboratory tests of low-cohesion granular materials 7 to 70 percent solid indicate that a plot of bearing capacity  $p$  against percentage of solid  $s$  (12) can be fitted, within a scatter of 10 percent in  $s$ , by the relation

$$s = 20 \log p/p_0 \quad (1)$$

where  $p_0 = 0.016$  newton/cm<sup>2</sup>. These tests used probes 0.6 to 2.8 cm in diameter under terrestrial gravity; cohesion of the materials tested was  $< 0.2$  newton/cm<sup>2</sup>. In the terrestrial tests for loosely packed material, with  $s \leq 50$  percent, the bearing stress varied directly as the depth for fixed width; the plotted  $p$  was taken at a width-to-depth ratio of 1 (12, 13). Analysis for loosely packed material indicated that  $p$  should be independent of the gravitational acceleration (13) and should be only slightly dependent on bearing width (14). For densely packed material ( $s > 50$  percent), the bearing capacity was reached at a small depth (high width-to-depth ratio), and the bearing stress increased very little with further increase in depth (13). For such material, analysis indicated that most of the bearing capacity would be provided by cohesion for bearing widths  $D$  (in centimeters) up to

$$D = 4 \times 10^4 c/g \quad (2)$$

where  $c$  is the cohesion (in newtons per square centimeter) and  $g$  is the gravitational acceleration (in centimeters per second per second) (13).

SCIENCE, VOL. 164

Table 1. Bearing capacity of lunar surface material and derivation of density.

Object	Imprint depth (cm)	Observed static bearing capacity (newton/cm <sup>2</sup> )	Bearing width (cm)	Ratio of width to depth	If loosely packed		If densely packed		Derived percentage of solid	Derived bulk density (g/cm <sup>3</sup> )
					Bearing capacity adjusted for depth (newton/cm <sup>2</sup> )	Solid (%)	Bearing capacity adjusted for gravity and width (newton/cm <sup>2</sup> )	Solid (%)		
Rolling stone	0.1	0.1	~1	~10	1	36	0.1	(16)	36	1.1
Alpha-scattering head	0.1-0.2	0.2	~1	5-10	1-2	36-42	0.2	(22)	36-42	1.2
Landing block	~2	1.8	18	~9	16	(60)	3.6	47	47	1.4
Surface sampler, Surveyor 7	2.0	1.6	2.5	0.8	1.3	38	1.6	40	38-40	1.2
Surface sampler, Surveyor 3	2.5	2	2.5	1	2	42	2	42	42	1.3
Footpad penetration	5	5.5	30	6	33	(64)	11	57	57	1.7
Rolling boulder	75	40	650	9	350	(86)	>4.4	>49	>49	>1.5

In this range,  $p$  would be independent of  $g$  and of width (13). At greater widths, most of the bearing capacity is provided by internal friction, and  $p$  would vary as  $gD$ .

It was not clear for each observation whether the lunar material behaved as though it was loosely packed or densely packed. Two separate calculations of the percentage of solid were made, one on the assumption that packing was loose and the other on the assumption that packing was dense. Equation 1 was used, with the observed lunar bearing capacity first adjusted to the appropriate terrestrial test conditions as follows: (i) For loose packing,  $p$  was adjusted for depth by multiplying by the lunar width-to-depth ratio divided by the width-to-depth ratio in the terrestrial tests. (ii) For dense packing,  $p$  was considered independent of  $gD$  up to a width of 12 cm and proportional to  $gD$  for larger widths. The 12-cm value was derived from Eq. 2 with  $g = 160 \text{ cm/sec}^2$  and  $c = 0.05 \text{ newton/cm}^2$ , a cohesion value measured at depths of a few centimeters on the

moon by several techniques (1, 9, 10, 15). For the boulder depth (75 cm),  $c$  was probably higher than 0.05 newton/cm<sup>2</sup>, so only a lower limit to the adjusted  $p$  was derived.

Columns 5 to 8 of Table 1 show the adjusted bearing capacity and the percentage of solid derived for each of these assumptions. Percentages of solids inconsistent with the assumed packing are shown in parentheses, and were disregarded. Column 9 shows the appropriate percentage of solid. The density of the solid material at the surface is close to 3 g/cm<sup>3</sup>; thus the percentage of solid was multiplied by this value to give the bulk density shown in the last column. Results are plotted in Fig. 2. A straight line, through 1.1 g/cm<sup>3</sup> at the surface and 1.6 g/cm<sup>3</sup> at a depth of 5 cm, fits the density points within uncertainty limits.

Prior to spacecraft landings on the moon, Matveev *et al.* (16) proposed two models of the density-depth relation for lunar material that would fit Earth-based radar, radio emission, and infrared emission measurements. One

model postulated a density at the surface of 0.6 g/cm<sup>3</sup>, with an exponential increase to about 1.0 g/cm<sup>3</sup> at a depth of 4 cm, a constant value of 1.0 g/cm<sup>3</sup> for several meters, and then a rather abrupt increase to solid or near solid rock at 7 to 15 m. The other model was similar but proposed a surface density of 1.0 g/cm<sup>3</sup>, with an increase to about 1.6 g/cm<sup>3</sup> at a depth of 4 cm (Fig. 2). Almost all of the later density-depth models have been in agreement with one or the other of the Matveev models (17).

The denser Matveev exponential model provides a reasonable fit to the densities obtained in this work, though not as good as a linear relation (Fig. 2). Scott's interpretation of the results of the Surveyor surface sampler (5) is also in reasonable agreement, but the data from Luna 13 are not.

One qualification should be noted: The terrestrial tests, on which Eq. 1 is based, were made with convex, solid particles, as ordinarily found in Earth soils and produced by comminution. The particles of the lunar surface are

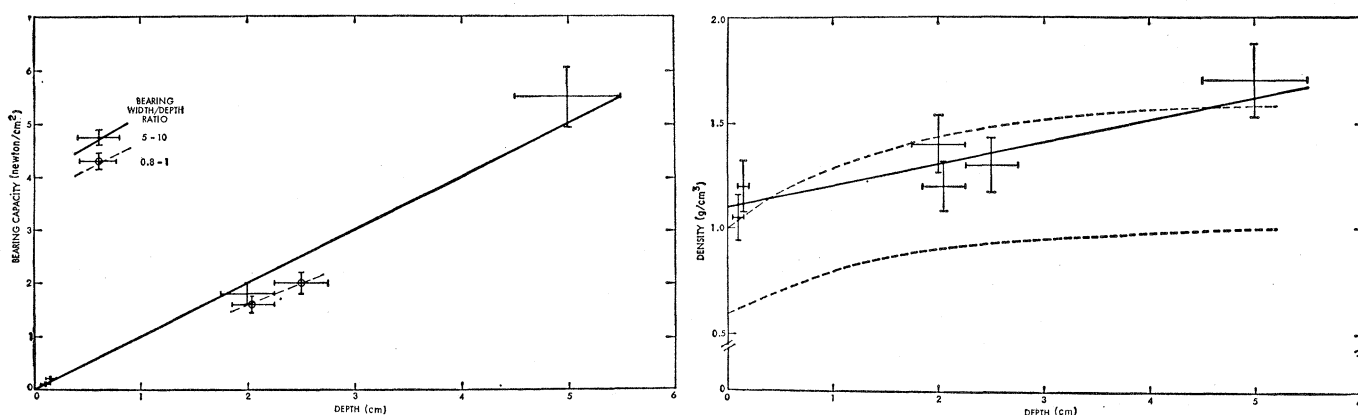


Fig. 1 (left). Static bearing capacity of lunar fragmental layer as a function of depth. Bars suggest uncertainty limits. Fig. 2 (right). Bulk density of lunar fragmental layer as a function of depth. Straight line fit (—); Matveev models (---). Bars suggest uncertainty limits.

predominantly 2 to 60  $\mu\text{m}$  in diameter (18) and have not been visually resolved in this size range; if they are porous or have concave surfaces that can interlock, the above findings may not be valid.

LEONARD D. JAFFE

Jet Propulsion Laboratory,  
California Institute of Technology,  
Pasadena 91103

#### References and Notes

- R. F. Scott and F. I. Roberson, *NASA (Nat. Aeronaut. Space Admin.) SP-173* (1968), pp. 121-161.
- A. L. Turkevich, E. J. Franzgrote, J. H. Patterson, *Science* **162**, 117 (1968).
- D. E. Gault, J. B. Adams, R. J. Collins, G. P. Kuiper, H. Masursky, J. A. O'Keefe, R. A. Phinney, E. M. Shoemaker, *NASA (Nat. Aeronaut. Space Admin.) SP-173* (1968), pp. 233-276.
- I. I. Cherkasov, A. L. Kemurjian, L. N. Mikhailov, V. V. Mikheyev, A. A. Morozov, A. A. Musatov, I. A. Savenko, M. I. Smorodinov, V. V. Shvarev, *Kosm. Issled. Akad. Nauk SSSR* **5**, 746 (1967) [translated in *Cosmic Res.* **5**, 636 (1967)]; A. A. Morozov, M. I. Smorodinov, V. V. Shvarev, I. I. Cherkasov, *Dokl. Akad. Nauk SSSR* **179**, 1087 (1968) [*Soviet Phys. Dokl. Engl. Transl.* **13**, 348 (1968)].
- R. F. Scott, *J. Geophys. Res.* **73**, 5469 (1968).
- Yu. A. Surkov, personal communication.
- E. M. Shoemaker, R. M. Batson, H. E. Holt, E. C. Morris, J. J. Rennison, E. A. Whitaker, *NASA (Nat. Aeronaut. Space Admin.) SP-163* (1967), pp. 9-42.
- R. Choate, S. A. Batterson, E. M. Christensen, R. E. Hutton, L. D. Jaffe, R. H. Jones, H. Y. Ko, R. L. Spencer, F. B. Sperling, *NASA (Nat. Aeronaut. Space Admin.) SP-173* (1968), pp. 83-119.
- E. M. Christensen, S. A. Batterson, H. E. Benson, R. Choate, R. E. Hutton, L. D. Jaffe, R. H. Jones, H. Y. Ko, F. N. Schmidt, R. F. Scott, R. L. Spencer, F. B. Sperling, G. H. Sutton, *NASA (Nat. Aeronaut. Space Admin.) SP-166* (1968), pp. 41-95.
- R. F. Scott and F. I. Roberson, *J. Geophys. Res.* **73**, 4045 (1968).
- A. L. Filice, *Science* **156**, 1486 (1967).
- L. D. Jaffe, *J. Geophys. Res.* **70**, 6268 (1965).
- E. C. Bennett, R. F. Scott, L. D. Jaffe, E. P. Frink, H. E. Martens, *AIAA (Amer. Inst. Aeronaut. Astronaut.) J.* **2**, 94 (1964).
- I. I. Cherkasov, in *Proceedings of the Geotechnical Conference Oslo* (Norwegian Geotechnical Institute, Oslo, Norway, 1967), vol. 1, pp. 179-180.
- E. M. Christensen, S. A. Batterson, H. E. Benson, R. Choate, R. E. Hutton, L. D. Jaffe, R. H. Jones, H. Y. Ko, F. N. Schmidt, R. F. Scott, R. L. Spencer, G. H. Sutton, *NASA (Nat. Aeronaut. Space Admin.) SP-163* (1967), pp. 43-87.
- Yu. G. Matveev, G. L. Suchkin, V. S. Troitskii, *Astron. Zh.* **42**, 810 (1966) [*Soviet Astron. AJ Engl. Transl.* **9**, 626 (1966)].
- L. D. Jaffe, *Icarus* **6**, 75 (1967); *J. Geophys. Res.* **72**, 1727 (1967); E. M. Christensen, S. A. Batterson, H. E. Benson, C. E. Chandler, R. H. Jones, R. F. Scott, E. N. Shipley, F. B. Sperling, G. H. Sutton, *ibid.*, p. 801; E. M. Christensen, S. A. Batterson, H. E. Benson, R. Choate, L. D. Jaffe, R. H. Jones, H. Y. Ko, R. L. Spencer, F. B. Sperling, G. H. Sutton, *J. Geophys. Res.* **73**, 4081 (1968); J. W. Salisbury and J. E. M. Adler, *Icarus* **7**, 243 (1967); L. D. Jaffe, S. A. Batterson, W. E. Brown, Jr., E. M. Christensen, S. E. Dwornik, D. E. Gault, J. W. Lucas, R. H. Norton, R. F. Scott, E. M. Shoemaker, R. H. Steinbacher, G. H. Sutton, A. L. Turkevich, *NASA (Nat. Aeronaut. Space Admin.) SP-166* (1968), pp. 1-3; M. J. Campbell, J. Ulrichs, T. Gold, *Science* **159**, 973 (1968); B. P. Jones, *J. Geophys. Res.* **73**, 7631 (1968); L. D. Jaffe, S. A. Batterson, W. E. Brown, Jr., E. M. Christensen, D. E. Gault, J. W. Lucas, R. H. Norton, R. F. Scott, E. M. Shoemaker, G. H. Sutton, A. L. Turkevich, *J. Geophys. Res.* **73**, 3983 (1968).
- E. M. Christensen, S. A. Batterson, H. E. Benson, R. Choate, R. E. Hutton, L. D. Jaffe, R. H. Jones, H. Y. Ko, F. N. Schmidt, R. F. Scott, R. L. Spencer, G. H. Sutton, *J. Geophys. Res.* **73**, 7169 (1968); L. D. Jaffe, *Science* **164**, 775 (1969).
- This paper presents the results of one phase of research carried out at the Jet Propulsion Laboratory, California Institute of Technology, under NASA contract NAS7-100.

9 May 1969

## Fission Track Age of Magnetic Anomaly 10:

### A New Point on the Sea-Floor Spreading Curve

**Abstract.** *A portion of basaltic glass retrieved from an abyssal hill in the northeast Pacific has been dated by the fission track method. The sample location corresponds to magnetic anomaly 10 believed to have resulted from sea-floor spreading. The age of this sample is  $35 \pm 5$  million years, which is in agreement with the previously proposed age of 31 to 32 million years based on linear extrapolation of measured recent spreading rates. This observation upholds the suggestions of other authors on the time variation of sea-floor spreading for the last 30 million years in various parts of the world ocean basin.*

Several kilograms of basalt of tholeiitic composition (1) have been recovered from an abyssal hill in the northeast Pacific near  $32^{\circ}25'N$ ,  $125^{\circ}38'W$ . The sample was recovered during expedition Tow Más aboard the research vessel *Thomas Washington* of the Scripps Institution of Oceanography. The hill is elongate north-south, with a flat top and steep linear scarps for its sides. It resulted primarily from post-depositional faulting of the oceanic

crust (2). The sample was dredged from depths of 4400 to 4300 m off a scarp 100 m high on the east side of the hill. Near-bottom seismic data showed that the scarps on the hillsides are devoid of sediment (2). The rock exposed on the scarp is either the original oceanic crust or volcanic outpourings that accompanied the faulting. This hill is located in an area of linear magnetic anomalies believed to have resulted from sea-floor spreading processes. The

sample has been taken from the younger positive event of anomaly 10 (3) as defined by Pitman *et al.* (4).

The ages of the younger magnetic anomalies, up to anomaly 3, are known by comparison with potassium-argon dates of rocks of known magnetic polarity within the interval 0 to 4.5 million years (5). Based on these ages, the recent spreading rate of oceanic rises has been determined in many parts of the world ocean basin (6). However, because the ages of anomalies beyond number 3 (~4 million years) have not been determined, an estimation of the early Tertiary spreading rates is not possible. Heirtzler *et al.* (7) have done the opposite by using a marine magnetic profile from the South Atlantic (V-20, S.A.), which they suggest by a series of arguments represents a record of linear spreading. They dated the anomalies by extrapolating the measured recent rate back in time. The age of the younger positive event of anomaly 10 by their time scale is from 31.50 to 31.84 million years. It was decided to date the present sample to determine if its age was concordant with the linear extrapolation of Heirtzler *et al.* (7). If the rock turned out to be younger than about 30 million years it could be dismissed as a recent geologic event, such as a fragment of a lava flow which issued from the fault scarp. If it proved older than the proposed age, the long-term sea-floor spreading rate for V-20 S.A. could be interpreted as being lower than the proposed rate and non-linear. Then the proposed ages of marine magnetic anomalies (7) would have to be revised upward. If the ages were in accordance, then the hypothesis is upheld in this one test, but it is not proved.

Petrographic examination of thin sections of the rock (1) indicated that it was unsuitable for potassium-argon dating. The samples possess a glassy crust, 1 to 7 mm thick, that is relatively unweathered. However, recent studies have shown that basaltic glass crusts from rocks dredged at this depth often show large amounts of excess argon (8), so that quenched glass is also unsuitable for potassium-argon dating. The fission track method is therefore uniquely applicable for the age determination of this sample.

Fission track dating of authigenic deep-sea glasses has been described previously (9). In the work described here, we isolated samples of the glass crust, 0.1  $\text{cm}^2$  in area, potted them in